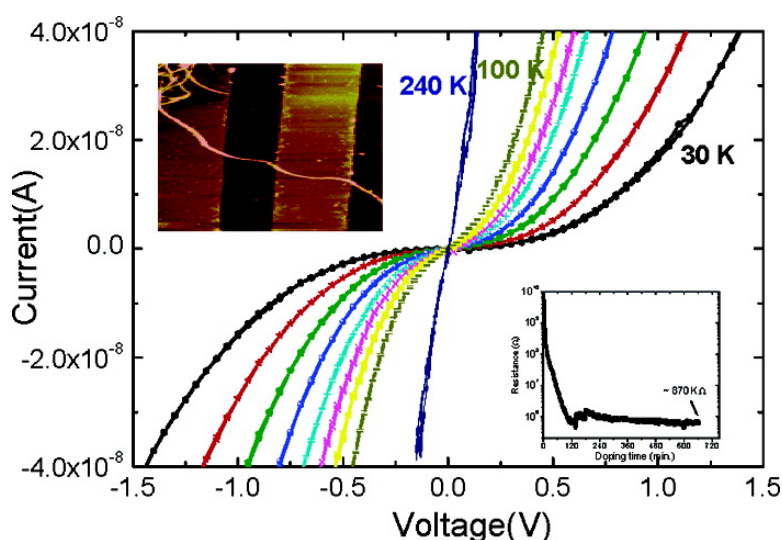


Dispersion and Current–Voltage Characteristics of Helical Polyacetylene Single Fibers

Hyun J. Lee, Zhao X. Jin, Andrey N. Aleshin, Ju Y. Lee, Mun J. Goh, Kazuo Akagi, Young S. Kim, Dong W. Kim, and Yung W. Park

J. Am. Chem. Soc., **2004**, 126 (51), 16722-16723 • DOI: 10.1021/ja044615y • Publication Date (Web): 02 December 2004

Downloaded from <http://pubs.acs.org> on April 5, 2009



More About This Article

Additional resources and features associated with this article are available within the HTML version:

- Supporting Information
- Links to the 4 articles that cite this article, as of the time of this article download
- Access to high resolution figures
- Links to articles and content related to this article
- Copyright permission to reproduce figures and/or text from this article

[View the Full Text HTML](#)

Dispersion and Current–Voltage Characteristics of Helical Polyacetylene Single Fibers

Hyun J. Lee,[†] Zhao X. Jin,[‡] Andrey N. Aleshin,^{†,§} Ju Y. Lee,[†] Mun J. Goh,^{||} Kazuo Akagi,^{||}
Young S. Kim,[†] Dong W. Kim,[†] and Yung W. Park^{*,†}

School of Physics and Nano Systems Institute-National Core Research Center, Seoul National University, Seoul, 151-747, Korea, Department of Chemistry, Renmin University of China, Beijing, PR China, A. F. Ioffe Physical-Technical Institute, Russian Academy of Sciences, St. Petersburg 194021, Russia, and Institute of Material Science, Tsukuba Research Center for Interdisciplinary Materials Science (TIMS), University of Tsukuba, Tsukuba, Ibaraki 350-8573, Japan

Received September 5, 2004; E-mail: ywpark@phy.snu.ac.kr

The synthesis and electronic properties of conducting polymer nanowires are the subject of intense interest in recent years due to potential applications in semiconductor nanotechnology.^{1–3} Many of these applications in nanoscale have been limited because of the lack of a method for obtaining a single fiber. The development of effective dispersion methods is crucial for substantial applications of conducting polymer fibers in the same manner as was done for single-walled carbon nanotubes.^{4,5} Only the problem of transport in a polymer fiber attracted significant attention mainly related to polyaniline fibers.^{6,7} Polyacetylene (PA) is the model conducting polymer showing an extremely high conductivity after doping.^{8–10} Recently, a novel helical PA was introduced by Akagi et al.¹¹ Since it has planar chiral structures, unique magnetic and optical properties, such as molecular solenoid, were expected in this material. Despite the helical structure of chiral bulk film, the solenoid current without coating with any insulator layer is hardly produced because the helical bulk material is composed of tightly entangled ropes consisting of several fibers. However, on molecular level or nanometer scale the electric current of a doped helical PA single fiber might raise an induced magnetic field. To study the fiber properties on nanoscale, it is necessary to extract a single helical PA fiber.

In this communication, we report a new method designed to obtain well-dispersed helical PA single fibers. We use an organic solution with a nonionic surfactant. Atomic force microscopy (AFM) imaging is performed to monitor the helical fibrillar structures of extracted single fibers, and the current–voltage (I – V) characteristics of iodine-doped helical PA fibers are investigated.

Helical PA is synthesized using chiral nematic liquid crystals (LCs) as a solvent of Ziegler–Natta catalyst, which is presented elsewhere.¹¹ There are two types of helical films, R-helical PA (R-PA) and S-helical PA (S-PA). The direction of helicity of R-PA is counterclockwise and that of S-PA is clockwise in the form of entangled ropes as is evident from the scanning electron microscopy.^{11,12} Because of that it is difficult to separate one single fiber from the ropes. Therefore, a strong force, which overcomes the van der Waals force between the fibers, is required. To obtain a single fiber effectively, hexaethylene glycol mono-*n*-dodecyl ether ($C_{12}E_6$)¹³ was used as a nonionic surfactant in *N,N*-dimethylformamide (DMF) solution. The organic solution, DMF, enables prevention of possible aging effects in aqueous solution while $C_{12}E_6$ works as a stabilizing agent.

Table 1. Dispersion in Various $C_{12}E_6$ Concentrations

sampletype	$C_{12}E_6$ /DMF (g/L)	dispersion state
S-type	26.8	large aggregation after 2 days
	58.2	stable after 3 days
R-type	58.2	large aggregation after 2 days
	163.2	no visible aggregation after 3 days

A small piece of helical PA film is soaked in $C_{12}E_6$ /DMF and then is agitated by ultrasonication for several minutes. Well-dispersed helical PA fibers in solution showed the deep blue color, which is consistent with the transmission of light through *trans*-PA. To obtain this suspension, the proper concentration of $C_{12}E_6$ is important. The state of dispersion in various $C_{12}E_6$ concentrations is described in Table 1. No large or visible aggregation of dispersed S-PA fibers was observed in a proper concentration (58.2 g/L). Although the R-PA fibers are more tightly screwed compared with the S-PA fibers, the well-dispersed suspension of R-PA fiber can be acquired after increasing the concentration of $C_{12}E_6$ up to 163.2 g/L in DMF. The shape of these solutions remained the same after several days. To study the morphology of suspended helical PA fibers with AFM, a droplet of these suspensions was deposited onto the substrate and dried over 1 day under argon atmosphere. Figure 1 shows the AFM images of dispersed helical PA fibers. While the aggregation of entangled fibers is observed in the case of improper concentration (Figure 1a), the single fiber of the optimized suspension is well dispersed as shown in Figure 1, b and c. The vertical (horizontal) size of the cross-section is 30–70 nm (100–200 nm). This is much smaller than that of fiber observed from the SEM image of helical PA film.^{11,12} The typical length of our freshly prepared R- and S-PA fibers is of the order of 10 μ m. It was reported that in helical PA film the screw direction of the fibers is the same as of the chiral nematic liquid crystal (LC)s used as a solvent.^{12,14} This fact is supported by our AFM results, which show the periodic modulation in height along the single fiber due to the chiral structure of helical PA fiber (Figure 1d). As can be seen from Figure 1c,d, the main single fiber might consist of a few microfibrils with smaller diameter (refer the Supporting Information for more details).

Using well-dispersed helical PA fibers, the conductivity of the single fiber is measured. R-PA single fiber is deposited on top of a 2- μ m spacing electrode. Pt electrodes patterned by optical lithography are used to prevent chemical reaction with the dopant. The temperature dependencies of current–voltage characteristics are investigated with cryogenic displex-osp and Keithley 6517A.

Iodine doping is done in the gas phase up to the saturation level by monitoring the sample current. The doping was done right before

[†] Seoul National University.

[‡] Renmin University of China.

[§] Russian Academy of Sciences.

^{||} University of Tsukuba.

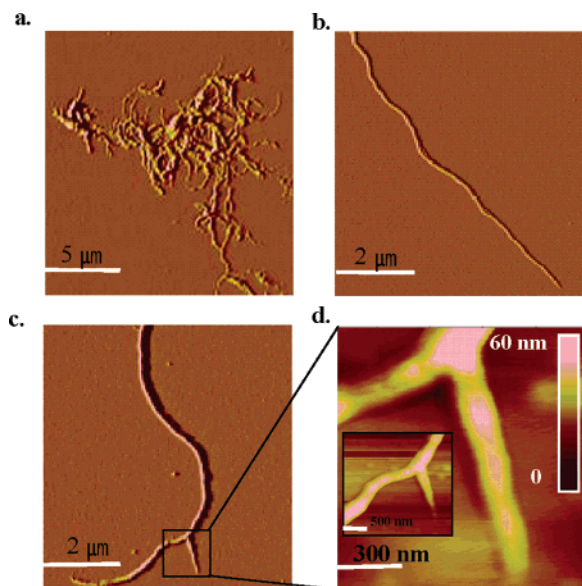


Figure 1. AFM images: (a) Dispersion in DMF without the surfactant. (b) Well-dispersed S-type (counterclockwise) and (c) R-type (clockwise) helical PA fiber. (d) Enlarged image of the square box; inset shows the scaled-down image.

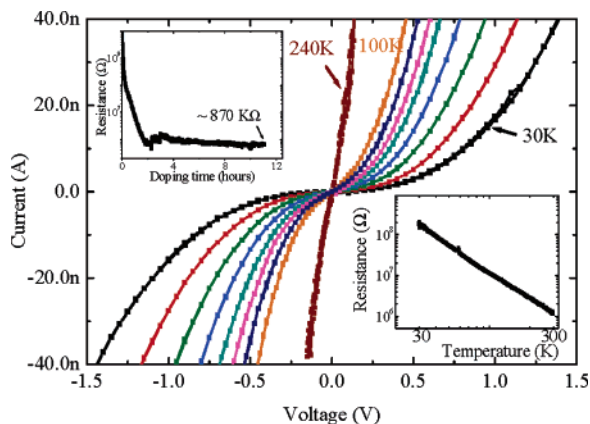


Figure 2. I - V characteristics of R-helical PA from 30 to 240 K. Left inset shows in situ doping with iodine. Right inset is the temperature dependence of resistance.

the transport measurements to minimize the aging effect. The left inset of Figure 2 shows the in situ doping with iodine measured at the 50 mV excitation voltage by two-probe-method. The resistance of helical PA fiber is decreased from several tens of $G\Omega$ down to $870\text{ K}\Omega$ after doping. The room-temperature conductance of a doped single fiber right before cooling is $\sim 8.4 \times 10^{-7}\text{ S}$ [the conductivity is equal to $\sim 1\text{ S/cm}$ with $\sim 65\text{ nm}$ (290 nm) of the vertical (horizontal) cross section and $2\text{ }\mu\text{m}$ length]. This conductance is lower than that of helical PA films¹⁵ but higher than that of conventional iodine-doped PA nanofiber,¹⁰ although the cis content of helical PA fiber is much less than that of PA nanofiber.¹⁶ This result demonstrates that the new method can be an effective way of dispersion without the aging effect. As the temperature decreases, the initially Ohmic I - V curve shows the nonlinear behavior. This trend becomes more significant below 240 K, as shown in Figure 2. The room-temperature conductance measurements of the sample in the Ohmic regime showed the values of the same order of magnitude in both two-probe and four-probe

geometry. It indicates that, despite the importance of contact resistance, the observed conductance is intrinsic to the quasi-one-dimensional (1D) helical PA fiber. The right inset of Figure 2 presents the temperature dependence of the resistance at 0.5 V excitation. The power-law behavior of $R(T)$ is well pronounced. We found that both hopping and 3D tunneling models did not fit our data well. This discrepancy might be related to the peculiarity of tunneling in such quasi-1D system as single helical PA fibers.¹⁷

In summary, we developed an effective dispersion method for helical PA fibers using a nonionic surfactant, $C_{12}E_6$. From the helical PA film we extracted single fibers through the optimized condition of $C_{12}E_6$ concentration in DMF solution. By using the AFM we have observed the structural features of well-dispersed single fibers. The current-voltage characteristics of helical PA single fibers are measured at various temperatures after iodine doping.

Acknowledgment. This work was supported by the Nano Systems Institute-National Core Research Center (NSI-NCRC) program of KOSEF, Korea. Z.X.J. and A.N.A. appreciated the support of BK21 Program of Korean Ministry of Education and Brain Pool Program of KFSTS, respectively.

Supporting Information Available: Experimental evidence and theoretical predictions of transport mechanism. This material is available free of charge via the Internet at <http://pubs.acs.org>.

References

- (1) Skotheim, T. A.; Elsenbaumer, R. L.; Reynolds, J. R. *Handbook of Conducting Polymers*, 2nd ed.; Marcel Dekker: New York, 1997.
- (2) (a) Huang, W. S.; Humphrey, B. D.; MacDiarmid, A. G. *J. Chem. Soc., Faraday Trans.* **1986**, *82*, 2385. (b) MacDiarmid, A. G. *Synth. Met.* **1997**, *84*, 27.
- (3) McGehee, M. D.; Heeger, A. J. *Adv. Mater.* **2000**, *12*, 1655.
- (4) Baughman, R. H.; Zakhidov, A. A.; de Heer, W. A. *Science* **2002**, *297*, 787.
- (5) (a) O'Connell, M. J.; Bachilo, S. M.; Huffman, C. B.; Moore, V. C.; Strano, M. S.; Haroz, E. H.; Rialon, K. L.; Boul, P. J.; Noon, W. H.; Kittrell, C.; Ma, J.; Hauge, R. H.; Weisman, R. B.; Smalley, R. E. *Science* **2002**, *297*, 593. (b) Islam, M. F.; Rojas, E.; Bergey, D. M.; Johnson, A. T.; Yodh, A. G. *Nano Lett.* **2003**, *3*, 269.
- (6) (a) Huang, J.; Virji, S.; Weiller, B. H.; Kaner, R. B. *J. Am. Chem. Soc.* **2003**, *125*, 314. (b) Huang, J.; Kaner, R. B. *J. Am. Chem. Soc.* **2004**, *126*, 851.
- (7) (a) MacDiarmid, A. G.; Jones, W. E.; Norris, I. D.; Gao, J.; Johnson, A. T.; Pinto, N. J.; Hone, J.; Han, B.; Ko, F. K.; Okuzaki, H.; Llaguno, M. *Synth. Met.* **2001**, *119*, 27. (b) Zhou, Y.; Freitag, M.; Hone, J.; Stail, C.; Jonson, A. T., Jr.; Pinto, N. J.; MacDiarmid, A. G. *Appl. Phys. Lett.* **2003**, *83*, 3800.
- (8) (a) MacDiarmid, A. G. *Rev. Mod. Phys.* **2001**, *73*, 713. (b) Heeger, A. J. *Rev. Mod. Phys.* **2001**, *73*, 701. (c) Shirakawa, H. *Rev. Mod. Phys.* **2001**, *73*, 713.
- (9) (a) Menon, R.; Yoon, C. O.; Moses, D.; Heeger, A. J. *Handbook of Conducting Polymers*, 2nd ed.; Dekker: New York, 1996. (b) Kohlman, R. S.; Joo, J.; Epstein, A. J. *Physical Properties of Polymers Handbook*; AIP: New York, 1996.
- (10) (a) Kim, G. T.; Burghard, M.; Suh, D.-S.; Kim, D. C.; Park, J. G.; Park, Y. W. *Synth. Met.* **1999**, *105*, 207. (b) Park, J. G.; Kim, B.; Lee, S. H.; Kaiser, A. B.; Roth, S.; Park, Y. W. *Synth. Met.* **2003**, *299*, 135. (c) Kaiser, A. B.; Park, Y. W. *Synth. Met.* **2003**, *245*, 135.
- (11) Akagi, K.; Piao, G.; Kaneko, S.; Sakamaki, K.; Shirakawa, H.; Kyotani, M. *Science* **1998**, *282*, 1683.
- (12) (a) Akagi, K.; Piao, G.; Kaneko, S.; Higuchi, I.; Shirakawa, H.; Kyotani, M. *Synth. Met.* **1999**, *102*, 1406. (b) Shirakawa, H. *Curr. Appl. Phys.* **2001**, *1*, 88.
- (13) Hexaethylene glycol mono-*n*-dodecyl ether, ($C_{12}E_6$, a common nonionic surfactant) $HO(CH_2CH_2O)_6(CH_2)_{11}CH_3 = 450.65$, was used as an assistant agent to produce a synergistic effect in stabilizing a colloidal system.
- (14) Piao, G.; Akagi, K.; Shirakawa, H.; Koytani, M. *Curr. Appl. Phys.* **2001**, *1*, 121.
- (15) Suh, D.-S.; Kim, T. J.; Aleshin, A. N.; Piao, G.; Akagi, K.; Shirakawa, H.; Qualls, J. S.; Han, S. Y.; Brooks, J. S.; Park, Y. W. *J. Chem. Phys.* **2001**, *114*, 7222.
- (16) Chien, J. C. W. *Polyacetylene*; Academic Press: New York, 1984.
- (17) Aleshin, A. N.; Lee, H. J.; Park, Y. W.; Akagi, K. *Phys. Rev. Lett.* **2004**, *93*, 196601.

JA044615Y